Journal of Optics

PAPER

Coherent control of light-pulse propagation in a Raman induced grating

IOP Publishing Journal of Optics
J. Opt. 19 (2017) 055501 (7pp) https://doi.org/10.1088/2040-8986/aa6498

Coherent control of light-pulse propagation in a Raman induced grating

V G Arkhipkin[1,2] and S A Myslivets[1,3]

[1] Kirensky Institute of Physics, Federal Research Center KSC SB RAS, 50, Akademgorodok, Krasnoyarsk 660036, Russia
[2] Laboratory for Nonlinear Optics and Spectroscopy, Siberian Federal University, Krasnoyarsk 660079, Russia
[3] Department of Photonics and Laser Technology, Siberian Federal University, Krasnoyarsk 660079, Russia

E-mail: avg@iph.krasn.ru

Received 13 December 2016, revised 27 February 2017
Accepted for publication 6 March 2017
Published 30 March 2017

Abstract
We study light-pulse propagation in a dynamically controllable periodic structure (grating) resulting from Raman interaction of a weak probe pulse with a standing-wave pump and a second control laser field in N-type four-level atomic media. The grating is induced due to periodic spatial modulation of the Raman gain in a standing pump field (Raman gain grating). We show that it is possible to control both the probe pulse amplitude and the group velocity of the pulse from subluminal to superluminal by varying the pump or control field. Such a grating is of interest for all-optical switches and transistors.

Keywords: light induced gratings, pulse propagation, Raman gain

(Some figures may appear in colour only in the online journal)

1. Introduction

The propagation of light in periodic structures has been an attractive field of research in recent years. Photonic crystals (PCs) represent a broad and special class of structures with a periodicity of the refractive index (the real part of the dielectric constant) on the wavelength scale in one, two, or three dimensions [1]. They have optical band gaps, which offer the possibility of controlling the propagation of light in a way similar to the control of electron flow in semiconductors. Additional functionality can be created by including absorbing or amplifying features into the structure, thus producing PCs with complex dielectric indices [2]. Creating reconfigurable PCs offers the opportunity of creating optically induced gratings [3]. In particular, such structures could be created by using electromagnetically induced transparency [4] when the strong-coupling laser field is replaced by a standing wave [5, 6]. A standing-wave driven configuration has been proposed to induce spatially periodic quantum coherence for the generation of photonic band gap structures [6–8] and dynamic generation of stationary light pulses [9, 10]. These structures are also referred to as an electromagnetically induced absorption grating (EIAG) [11]. EIAGs may be utilized for diffracting [12], switching [11] and compressing [13] the probe field. This scheme has also been used for atoms localizing in a standing-wave field [14, 15].

An alternative approach is based on using the Raman gain effect [16] in three- and four-level media where we can control the amplification of the probe (signal) field. It has been shown that slow [17] and fast [18] light as well as a gain-assisted giant Kerr effect [19] can be obtained by using a Raman gain medium. A fast Kerr phase gate using the Raman gain method has been experimentally demonstrated where the probe wave travels superluminally [20]. In our papers [21, 22] it was shown how one could use a three- and four-level Raman gain medium together with a PC cavity to create an all-optical switch for a probe beam. Recently, we proposed electromagnetically induced gratings based on the spatial modulation of the Raman gain in a standing-wave pump field [23, 24], which are called Raman induced gratings (RIGs). These gratings are fundamentally different from EIAG schemes where the absorption is spatially modulated. Owing to periodic spatial modulation of the Raman gain, the weak probe wave propagates in the forward (a transmitted

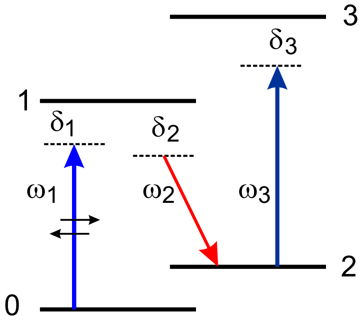

Figure 1. A schematic diagram of the four-level N-type atomic system for coherent manipulation of the probe (signal) light pulse. The pump field with frequency ω_1 is a standing wave. The probe field has a frequency ω_2, and ω_3 correspond to the control field. The frequency detuning $\delta_{1,2,3}$ denote the detunings from one-photon resonances for the pump, probe and control fields, respectively.

wave) and backward (a reflected wave) directions. In [23] it was shown that transmitted and reflected waves can be simultaneously amplified at a certain frequency band and the transmission and reflection spectra can be controlled (from amplification to suppression) by varying the pump field intensity. In [24] we showed that the transmission and reflection spectra of RIGs can be controlled with the help of an additional control field by varying its intensity or frequency. In this paper, we extend our previous results [23, 24] to further investigate the probe pulse propagation in such a grating. We show that it is possible to control both the amplitude of the probe pulse (with amplification or suppression) and the group velocity from subluminal to superluminal by varying the pump or control field. This structure can operate as an all-optical switch and a transistor.

2. Basic theory

A model for coherent control of the RIG is shown schematically in figure 1. It can be described by a four-level N-type configuration initially prepared in the ground state $|0\rangle$. The ground $|0\rangle$ and metastable $|2\rangle$ levels are coupled to the excited level $|1\rangle$ by a strong pump field at frequency ω_1 and a weak probe (signal) field at the frequency ω_2 and wave number k_2. A strong control field at frequency ω_3 and wave number k_3 is applied to the transition $|2\rangle - |3\rangle$ to enable manipulation by means of the Raman gain. The probe ($E_s = 1/2E_2\exp[-i(\omega_2 t - k_2 z)]$) and control ($E_c = 1/2E_3\exp[-i(\omega_3 t - k_3 z)]$) fields propagate along the z direction and interact with the transitions $|1\rangle - |2\rangle$ and $|2\rangle - |3\rangle$, respectively. The pump field is a standing wave along the z direction. It is formed by two monochromatic counter-propagating fields $E_p = 1/2\{E_{1+}\exp[-i(\omega_1 t - k_1 z)] + E_{1-}\exp[-i(\omega_1 t + k_1 z)]\}$, where E_{1+} and E_{1-} are the amplitudes of the forward (+) and backward (−) pump fields with the respective Rabi frequencies G_{1+} and G_{1-}. The pump fields are detuned from state $|1\rangle$ by large one-photon detuning so that single-photon absorption can be neglected. We assume that the Rabi frequency of the probe is much lower than the Rabi frequencies of the pump and control field, which are considered strong fields. The intensity of the pump radiation field is selected such that the threshold of stimulated Raman scattering is not exceeded, being, however, high enough to ensure notable amplification of the probe wave. At the same time, spontaneous Raman gain should be much less than the stimulated one.

The induced macroscopic polarization at the probe frequency ω_2 will be $P(\omega_2) = N\rho_{21}d_{12} = \chi(\omega_2)E_2$, where N is the atomic number density, and $\chi(\omega_2)$ is the Raman susceptibility. We assume that the fields are limited to a value such that the change of population of the ground level ρ_0 due to absorption to other levels under applied fields is small, i.e. $\rho_0 \approx 1$. The steady-state density matrix equations of motion for the four-level system under the dipole and rotating wave approximation can be written as

$$\begin{aligned}\Delta_2\rho_{21} &= iG_1^*\rho_{20} - iG_3^*\rho_{31}\\ \Delta_{20}\rho_{20} &= -iG_2^*\rho_{10} + \mathrm{i}\rho_{21}G_1 - iG_3^*\rho_{30}\\ \Delta_1\rho_{10} &= -iG_p\rho_0\\ \Delta_{30}\rho_{30} &= -iG_{32}\rho_{20} + \mathrm{i}\rho_{31}G_p\\ \Delta_{31}\rho_{31} &= -iG_3\rho_{21} + \mathrm{i}\rho_{30}G_p^*\end{aligned} \tag{1}$$

where $G_p = G_{1+}\exp(\mathrm{i}k_1 z) + G_{1-}\exp(-\mathrm{i}k_1 z)$, $G_{1\pm} = E_{1\pm}d_{10}/2\hbar$, $G_2 = E_2 d_{12}/2\hbar$, and $G_3 = E_3 d_{32}/2\hbar$ denote the Rabi frequencies of the pump, probe and control fields, respectively, $\Delta_1 = \gamma_{10} - \mathrm{i}\delta_1$, $\Delta_2 = \gamma_{12} - \mathrm{i}\delta_2$, $\Delta_3 = \gamma_{32} - \mathrm{i}\delta_3$, $\Delta_{30} = \gamma_{30} - \mathrm{i}\delta_{30}$, $\Delta_{31} = \gamma_{31} - \mathrm{i}\delta_{31}$, and $\delta_{1,2,3} = \omega_{1,2,3} - \omega_{10,12,32}$ are the one-photon detuning, $\delta_{20} = \delta_1 - \delta_2$ is the Raman detuning, $\delta_{30} = \delta_1 - \delta_2 + \delta_3$, $\delta_{31} = \delta_3 - \delta_2$; ω_{mn}, γ_{mn} and d_{mn} are the frequency, half-width and matrix dipole moment of the respective transitions; $\hbar$ is the reduced Planck constant. Equation (1) is valid if $|G_2| \ll |G_{1\pm}|$, $|G_3|$, $\delta_1 \gg \gamma_{10}$, $|G_{1\pm}|$.

The solution for the element ρ_{21} (to the first order in the probe field and to all orders in the pump and control fields) is

$$\rho_{21} = -i\frac{G_2}{\Delta_1}|G_p|^2(\Delta_{30}\Delta_{31} + |G_p|^2 - |G_3|^2)/D, \tag{2}$$

where

$$\begin{aligned}D = (|G_p|^2 - |G_3|^2)^2 + (\Delta_{20}|G_p|^2 + \Delta_{31}|G_3|^2)\Delta_2^*\\ + (\Delta_{31}|G_p|^2 + \Delta_{20}|G_3|^2)\Delta_{30} + \Delta_{30}\Delta_{20}\Delta_{31}\Delta_2^*.\end{aligned}$$

From (2), the susceptibility $\chi(\omega_2)$ experienced by the probe field can be written as

$$\chi(\omega_2) = -\mathrm{i}\frac{\alpha_r\gamma_{10}}{\Delta_1}|G_p|^2(\Delta_{30}\Delta_{31} + |G_p|^2 - |G_3|^2)/D, \tag{3}$$

where $\alpha_r = |d_{12}|^2 N/2\hbar\gamma_{10}$. When the control field is switched off ($G_3 = 0$), formula (3) is essentially simplified (see the appendix).

Further, we shall assume that the amplitudes of the pump field are real and $E_{1+} = E_{1-} = E_1$. In this case, the pump field is a perfect standing wave with the Rabi frequency $G_p(z) = G_1\cos(k_1 z)$, where $G_1 = E_1 d_{10}/\hbar$. Susceptibility (3), which depends on z through $|G_p(z)|^2 = G_1^2\cos^2(k_1 z) = G_1^2[1 + \cos(2k_1 z)]/2$, is an even periodical function. Thus, susceptibility for the probe field is modulated periodically in space with the period $\Lambda = \lambda_1/2$, where λ_1 is the wavelength of the pump field. This leads to spatial modulation of the Raman gain and the refractive index. Amplification takes place in the antinodes region of the standing wave, but there is no gain in the nodes. We called such a structure an RIG [23]. It should be emphasized that this grating is a hybrid one: an amplitude (gain) grating and a phase (refraction) one. Therefore, the probe field propagates in such a medium as in a one-dimensional (1D) periodic structure, i.e. it may propagate both in the forward (the transmitted wave), and backward (reflected wave) directions.

The wave equation for the probe field $E_2(z)$ in a spatially modulated medium with the susceptibility $\chi(\omega_2, z)$ in a frequency domain takes the form [25, 26]

$$\frac{\mathrm{d}^2 E_2(\omega_2, z)}{\mathrm{d}\, z^2} + k_2^2[1 + 4\pi\chi(\omega_2, z)]E_2 = 0, \tag{4}$$

where $k_2 = \omega_2/c$ is the vacuum probe wave number. The solution of (4) can be represented as a superposition of two waves propagating in opposite directions:

$$E_2(z) = A(z)\mathrm{e}^{\mathrm{i}k_2 z} + B(z)\mathrm{e}^{-\mathrm{i}k_2 z}, \tag{5}$$

where $A(z)$ and $B(z)$ are the amplitudes of the forward and backward probe waves, respectively. Using the cosine Fourier expansion $\chi(\omega_2, z) = \chi_0 + 2\sum_{n=1}^{\infty}\chi_n\cos(2nk_1 z)$ (χ is an even function) and the coupled mode analysis [26], we can find the amplitudes $A(z)$ and $B(z)$ [23]

$$A(z) = A_0\frac{s\cos s(L-z) + \mathrm{i}(\Delta k - \alpha)\sin s(L-z)}{s\cos(sL) + \mathrm{i}(\Delta k - \alpha)\sin(sL)} \tag{6}$$

$$B(z) = A_0\frac{\sigma\sin s(L-z)}{s\cos(sL) + \mathrm{i}(\Delta k - \alpha)\sin(sL)} \tag{7}$$

where $s = \sqrt{(\Delta k - \alpha)^2 - \sigma^2}$, $\alpha = 2\pi k_2\chi_0$, $\sigma = 2\pi k_2\chi_1$, and $\Delta k = k_1 - k_2$.

$$\chi_m(\omega_2) = (k_1/\pi)\int_0^{\pi/k_1}\chi(\omega_2, z)\cos(2mk_1 z)dz \tag{8}$$

In defining (6) and (7), we used χ_0 ($m = 0$) and χ_1 ($m = 1$), i.e. we restricted ourselves to two spatial harmonics and also used the boundary conditions $A(z = 0) = A_0, B(L) = 0$, where A_0 is the incident probe wave amplitude (no Fresnel reflection from the interface).

Let us introduce the amplitude coefficients of transmission (gain) $t(\omega_2, z = L) = A(\omega_2, L)/A_0$ and reflection $r(\omega_2, z = 0) = B(\omega_2, 0)/A_0$

$$t(\omega_2) = \frac{s\cos(sL)}{s\cos(sL) + \mathrm{i}(\Delta k - \alpha)\sin(sL)}, \tag{9}$$

$$r(\omega_2) = \frac{\sigma\sin(sL)}{s\cos(sL) + i(\Delta k - \alpha)\sin(sL)}. \tag{10}$$

Then we can easily obtain the energy transmittance $T = |t(\omega_2)|^2$ and reflectance $R = |r(\omega_2)|^2$.

3. Results and discussion

For numerical simulations we use the parameters corresponding to the $D1$ line of Na atoms, and the levels $|0\rangle$ and $|2\rangle$ are long-lived hyperfine sublevels of the electronic ground state $3S_{1/2}$. The atomic parameters are $\gamma_{10} = 2\pi \times 10$ MHz, $\gamma_{20} = \gamma_{10}/100$, and $N = 10^{12}$ cm^{-3}, and the sample length is $L = 5$ mm. The Rabi frequency of the pump (G_1) and control (G_3) fields will be expressed in the units of γ_{10} and the Raman detuning δ_{20} in γ_{20} units.

3.1. The transmission and reflection spectra

Let us first consider the case when the control field is switched off ($G_3 = 0$). In figure 2 the transmission T and reflection R for the probe field are plotted as functions of the Raman detuning δ_{20} and pump Rabi frequency G_1 at a fixed one-photon detuning $\delta_1 = -100\gamma_{10}$. It can be seen that the transmission and reflection spectra strongly depend on the pump field intensity. The transmitted and reflected light can be amplified in some frequency range. Therefore, transmittance and reflectivity can be interpreted as a transmission and reflection gain, respectively. The transmission spectra depend on the Raman detuning δ_{20} and have a resonance character at the pump Rabi frequency. As the pump field intensity increases, there occurs a dip in the transmission spectrum near the Raman resonance. The depth and width of the dip increase with the pump intensity and the dip center is shifted due to the Stark shift of the resonance frequency of the Raman transition (see (A.1) in appendix). In the area between the peaks the sample may become opaque ($T \to 0$). A similar behavior also holds for reflection, but the dip is less pronounced. Away from the Raman resonance, the gain disappears ($T \to 1$ and $R \to 0$). Thus, by changing the intensity of the pump field we can control the transmission (reflection) spectrum of the probe radiation under Raman interaction with a standing-wave pump.

The presence of an additional control field (ω_3 in figure 1) leads to essential modification of the propagation properties of the medium [24]. The typical transmission spectrum is shown in figure 3 as a function of the Raman detuning δ_{20} and the control field Rabi frequency G_3. It is seen that the transmission has a resonant character as a function of G_3, i.e. a peak occurs at certain values of G_3, and its position depends on the intensity of the pump field. The intensity of the control field decreases with increasing thickness of the sample L. Note that small variations of the control field intensity can change the system from opaque to transparent (with amplification) and vice versa. In [24] it is shown that in the case of a non-perfect standing pump wave with unequal amplitudes for forward and backward fields, the transmission and reflection spectra qualitatively have the same behavior. In addition, although they are sensitive to the difference between the amplitudes of contradirected pump waves, this is not critical and does not lead to noticeable changes in the discussed dependencies. A similar behavior occurs for the reflection spectrum.

3.2. Control of light-pulse propagation

Using equations (9)–(10) and the Fourier transform method one can study the propagation dynamics of an incident probe pulse assuming that the pump standing wave and the control field are continuous and monochromatic waves. Here, we

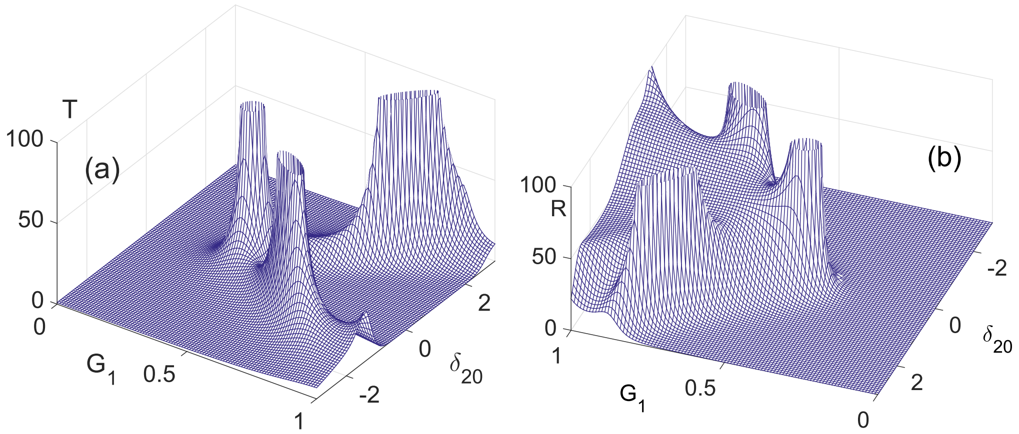

Figure 2. The transmission (a) and reflection (b) versus Raman detuning δ_{20} (in γ_{20} units) and pump Rabi frequency G_1 (in γ_{10} units) in the case when the control field is off ($G_3 = 0$).

assume that the input probe pulse has the following Gaussian profile in the time and frequency domains

$$E_{2\mathrm{i}}(t) = E_0 \exp(-t^2/\tau^2)$$
$$E_{2\mathrm{i}}(\omega_2) = 2^{-1/2}\tau E_0 \exp[-\tau^2(\omega_2 - \omega_{2\mathrm{c}})^2/4],$$

where E_0 is the pulse amplitude, 2τ is the pulse width at the level e^{-1}, $\omega_{2\mathrm{c}}$ is the carrier frequency of the probe pulse. The transmitted and reflected Fourier components can be derived from $E_{2\mathrm{T}}(\omega_2) = t(\omega_2)E_{2\mathrm{i}}(\omega_2)$ and $E_{2\mathrm{R}}(\omega_2) = r(\omega_2)E_{2\mathrm{i}}(\omega_2)$. The transmitted and reflected probe pulse in the time domain via inverse Fourier transform is given by

$$E_{2\mathrm{T},2\mathrm{R}}(t) = \int_{-\infty}^{\infty} E_{2\mathrm{T},2\mathrm{R}}(\omega_2)\exp(-\mathrm{i}\omega_2 t)\,\mathrm{d}\omega_2. \qquad (11)$$

Let us first consider the case $G_3 = 0$, i.e. the control field is off. Figure 4 shows the typical behavior of the transmitted ($z = L$) and reflected ($z = 0$) probe pulse for different values of the pump Rabi frequency G_1 under Raman resonance for the carrier frequency of the pulse ($\delta_{2\mathrm{c}} = \omega_1 - \omega_{2\mathrm{c}} - \omega_{20} = 0$). One can see that the transmitted and reflected pulses are sensitive to G_1. When the Rabi frequency G_1 corresponds to the left branch of the curve $T(G_1)$ (inset in figure 4(a)), the transmitted pulse is amplified and enhances with increasing G_1 (figure 4(a)). In the case when G_1 corresponds to the right branch of the curve $T(G_1)$, the pulse amplification decreases with increasing G_1 (figure 4(b)). A similar behavior also takes place for the reflected pulses (figure 4(c)). Thus, the RIG can operate as an all-optical switch and an amplifier. A similar pattern is observed for other detunings δ_{2c}.

We also note that the transmitted (reflected) pulse may either lag (figures 4(a) and (c)) or lead (figure 4(b)) the reference pulse (not shown), which covers the same distance in a vacuum. Therefore, we can speak about subluminal propagation of the probe pulse, when the pulse group velocity is less than the speed of light in vacuum (a slow light), or superluminal propagation, when the group velocity is negative or higher than the speed of light in vacuum (fast light) [27].

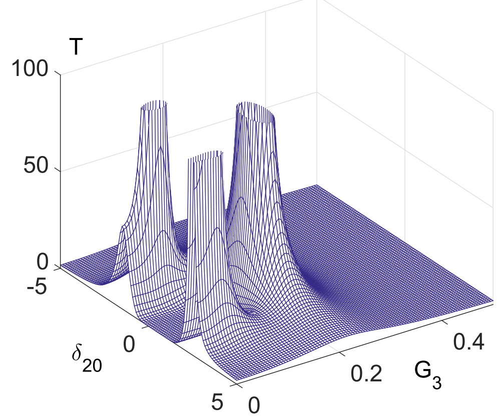

Figure 3. The transmission spectrum versus Raman detuning δ_{20} and control Rabi frequency G_3 (in γ_{10} units) for the case when the pump Rabi frequency $G_1 = 0.8$, and and the frequency detuning of the control field $\delta_3 = 0$.

Group delay for the transmitted and reflected pulse can be calculated as [28]

$$\tau_g^{\mathrm{T,R}} = \left(\frac{\partial\Phi_{\mathrm{T,R}}}{\partial\omega_2}\right)_{\omega_2=\omega_{2c}}$$

where $\Phi_{T,R}$ is the phase of the transmission $t(\omega_2)$ and reflection $r(\omega_2)$ coefficient, respectively. A positive group delay (the pulse at the output appears later than the reference) corresponds to the subluminal propagation. A negative group delay (the pulse at the output appears earlier than the reference) corresponds to the superluminal propagation. The inset in figure 5 shows the group delay τ_g as a function of the detuning δ_{20} for the values G_1 corresponding to the curves 3 (figure 4(a)) and 2 (figure 4(b)). In the first case ($G_1 = 0.31$) $\tau_g > 0$ (subluminal propagation) and in the second case ($G_1 = 0.45$) $\tau_g < 0$ (superluminal propagation). Calculations show that subluminal propagation occurs when the Rabi frequency G_1 corresponds to the left branch of the dependence $T(G_1)$ (see the inset in figure 4(a)), where normal dispersion for the probe wave is realized (figure 5). When G_1

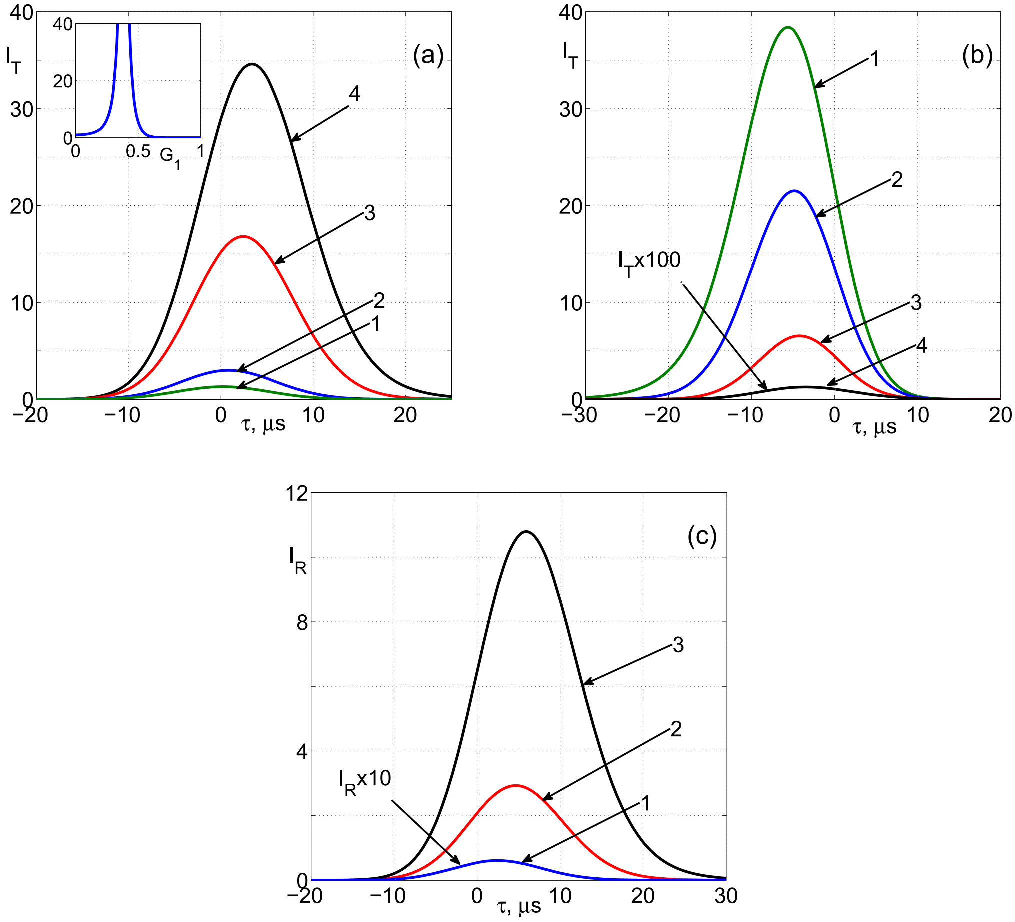

Figure 4. The transmitted I_T (a), (b) and reflected I_R (c) probe light pulse for different values of the Rabi frequency G_1 in the case when $G_3 = 0$, $\delta_{2c} = 0$. (a) 1 – $G_1 = 0.1$, 2 – $G_1 = 0.2$, 3 – $G_1 = 0.31$, 4 – $G_1 = 0.34$; (b) 1 – $G_1 = 0.43$, 2 – $G_1 = 0.45$, 3 – $G_1 = 0.5$, 4 – $G_1 = 0.8$; (c) 1 – $G_1 = 0.2$, 2 – $G_1 = 0.31$, 3 – $G_1 = 0.34$. The maximum of the reference pulse (not shown) corresponds to $\tau = 0$. The inset shows transmission T as a function of the pump field Rabi frequency.

corresponds to the right branch of the dependence $T(G_1)$, superluminal propagation arises since dispersion for the probe wave becomes anomalous (figure 5). The mechanism of attaining normal and anomalous dispersion is associated with dispersion of the RIG (structural dispersion) rather than the Raman medium (material dispersion).

The presence of a control field opens new possibilities for manipulating the propagation dynamics of the probe pulse. Figure 6 illustrates the transmitted and reflected Gaussian probe pulse for various Rabi frequencies G_3 at different values of the pump Rabi frequency G_1 (the operating point). The pulse propagation dynamics depends essentially on the Rabi frequency G_3. Figures 6(a) and (b) show the transmitted and reflected probe pulses in the case when the Rabi frequency G_1 corresponds to the left branch of the curve $T(G_1)$ or $R(G_1)$, respectively. Selecting the intensity of the control field, we can suppress the reflected pulse. In this case, the RIG acts as a controllable amplifier for transmitted and reflected pulses. Note that here we deal with subliminal pulses ($\tau_g > 0$) and τ_g depends on G_3.

Figure 6(c) shows the case when the intensity of the pump field is selected such that transmittance of the grating is close to zero (at $G_3 = 0$). When the control field is turned on the pulse amplification increases with G_3 (curves 2 and 3 in figure 6(a)) as long as the Rabi frequency G_3 corresponds to the left branch of the curve $T(G_3)$ (the inset in figure 6(a)). When G_3 corresponds to the right branch, the pulse amplification decreases with increasing G_3. Meanwhile, the group

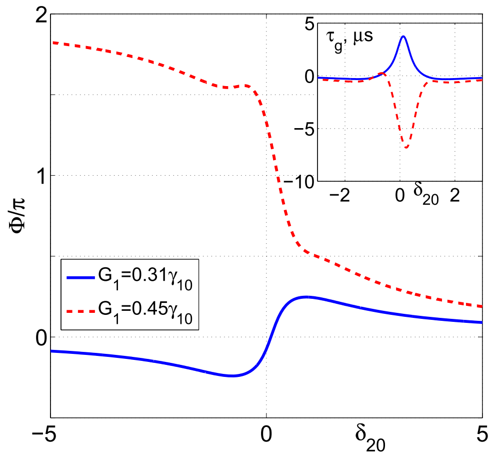

Figure 5. Spectral dependences of the phase of the transmitted probe wave for the Rabi frequencies $G_1 = 0.31$ and $G_1 = 0.45$. Inset: the group delay τ_g as a function of detuning from the Raman resonance δ_{2c} for the same G_1.

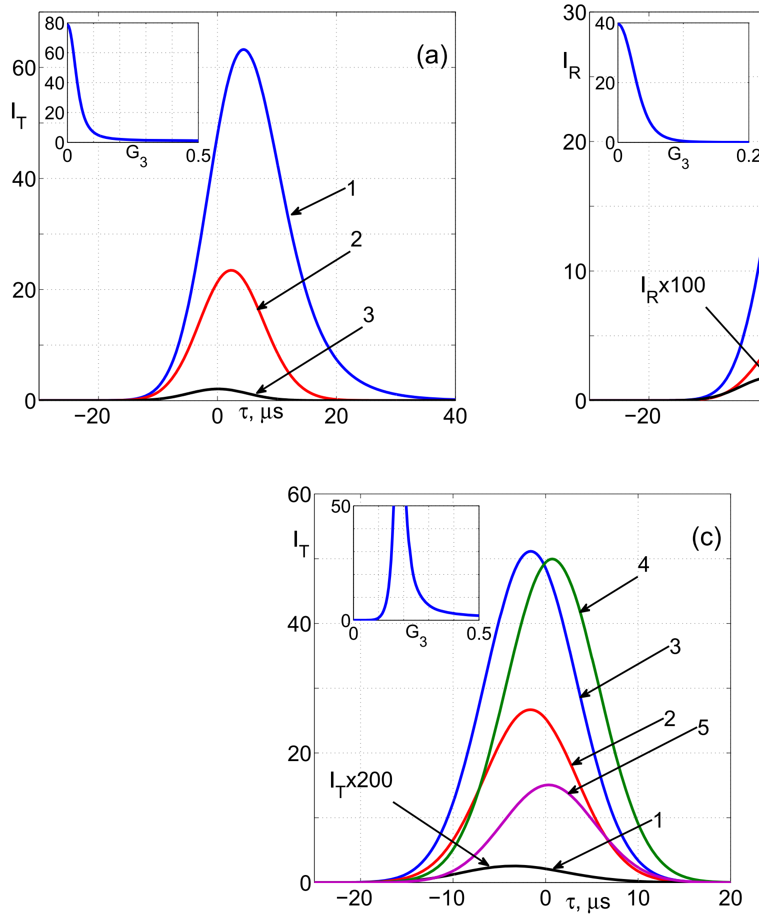

Figure 6. The transmitted (I_T) and reflected (I_R) probe light pulse for different values of the Rabi frequency G_1 and $\delta_{32} = 0$, $\delta_{2c} = 0$. (a), (b) $G_1 = 0.36$, 1 – $G_3 = 0$, 2 – $G_3 = 0.05$, 3 – $G_3 = 0.2$. (c) $G_1 = 0.8$, 1 – $G_3 = 0$, 2–$G_3 = 0.15$, 3 – $G_3 = 0.16$, 4 – $G_3 = 0.21$, 5 – $G_3 = 0.25$. The insets show the transmission T (a, c) and reflection R (b) as a function of the control field Rabi frequency G_3.

velocity of the pulse also changes from subluminal to superluminal. Thus, by changing the control field intensity we can change the system from opaque to transparent (with amplification) and vice versa, i.e. this structure can operate as an all-optical transistor.

4. Conclusion

We have presented a theoretical study on the probe light-pulse propagation under Raman interaction with a pump standing wave in three- and four-level media. For a three-level atomic system, we show that it is possible to control both the transmission (reflection) of the probe pulse and the dispersion of the RIG (structural dispersion) by changing the intensity of the pump field. In this way the dispersion can be changed from normal to abnormal, and we can therefore manipulate the pulse group velocity from subliminal to superluminal. We have also shown that by adding a control field coupled to a fourth state the properties of the weak probe light-pulse propagation are greatly changed. In particular small variations in the intensity of control field transfer the system from the opaque to transparent (with amplification) state and vice versa. Therefore this structure can operate as an all-optical transistor. At the same time, it can be used as a nonlinear controllable mirror with the reflectivity greater than unity. In addition, due to the variation of the control field intensity, the probe pulse propagation can be changed from subluminal to superluminal. This opens up new possibilities for manipulating the dispersion and transmission, and may be used in different fields of applied photonics.

The intensity of the control and pump field strongly depends on a number of parameters (detuning from one-photon and Raman resonances, a Raman resonance width, a sample thickness and others). The required laser field intensity is tens of hundreds of mW cm^{-2} for the pump field and two to three orders of magnitude lower for the control field.

Acknowledgments

This work was supported by the Russian Foundation for Basic Research under Grant No. 15-02-03959 and partially by the Siberian Branch of the Russian Academy of Sciences under Complex Program II.2P (0356-2015-0410).

Appendix

In the appendix, we give the formula for the susceptibility $\chi(\omega_2, z)$ for the case when the control field is off ($G_3 = 0$) and calculate the Fourier components (8) χ_0 and χ_1 in this case. It is not difficult to show that when $G_3 = 0$ and $|\delta_1| \gg \gamma_{10}$, $|\delta_2| \gg \gamma_{12}$ susceptibility (3) simplifies to

$$\chi(\omega_2, z) = \frac{\alpha_r \gamma_{10}}{\delta_1} \times \frac{G_1^2[1 + \cos(2k_1 z)]/2}{\delta_2[\delta_{20} + G_1^2/2\delta_2 + \mathrm{i}\gamma_{20} + G_1^2\cos(2k_1 z)/2\delta_2]}. \tag{A.1}$$

From equation (A.1) we see that a strong pump field ($G_1^2/|\delta_2| \gg \gamma_{20}$) causes a shift in the resonance frequency of the Raman transition (the Stark shift). In the case of a weak pump field ($G_1^2/|\delta_2| \ll \gamma_{20}$) equation (A.1) is consistent with the standard Raman susceptibility as defined in perturbation theory [16].

For susceptibility (A.1) the spatial Fourier components χ_0 and χ_1 are calculated analytically. To calculate integrals (8) for the $\chi(\omega_2, z)$, formula (A.1) is conveniently rewritten as

$$\chi(\omega_2, z) = \frac{\alpha_r \gamma_{10}}{\delta_1}\frac{A[1 + \cos(2k_1 z)]}{1 + A\cos(2k_1 z)}, \tag{A.2}$$

where $A = \frac{G_1^2}{2\delta_2}\frac{1}{\delta_{20} + G_1^2/2\delta_2 + \mathrm{i}\gamma_{20}}$.

Then

$$\chi_0 = \frac{k_1}{\pi}\frac{\alpha_r \gamma_{10}}{\delta_1} A \int_0^{\pi/k_1} \frac{1 + \cos(2k_1 z)}{1 + A\cos(2k_1 z)}\mathrm{d}z = \frac{\alpha_r \gamma_{10}}{\delta_1}\frac{1 - A + \sqrt{1 - A^2}}{1 + A} \tag{A.3}$$

$$\chi_1 = \frac{k_1}{\pi}\frac{\alpha_r \gamma_{10}}{\delta_1} A \int_0^{\pi/k_1} \frac{1 + \cos(2k_1 z)}{1 + A\cos(2k_1 z)}\cos(2k_1 z)dz = \frac{\alpha_r \gamma_{10}}{\delta_1}\frac{A^2 - 1 + \sqrt{1 - A^2}}{A(1 + A)}. \tag{A.4}$$

Numerical simulations using formula (8) with $G_3 = 0$ are in good agreement with the analytical results (A.3)–(A.4).

References

[1] Notomi M 2010 *Rep. Prog. Phys.* **73** 096501
[2] Rozanov N N, Fedorov S V, Savel'ev R S, Sukhorukov A A and Kivshar Y S 2012 *JETP* **114** 782
[3] Neshev D N, Sukhorukov A A, Mitchell A, Rosberg C R, Fischer R, Dreischuh A, Krolikowski W Z and Kivshar Y S 2007 *14th Int. Sch. Quantum Electron.: Laser Phys. Appl.* Vol 6604 (Proc. SPIE) pp 66041B–15
[4] Fleischhauer M, Imamoglu A and Marangos J P 2005 *Rev. Mod. Phys.* **77** 633
[5] Su X M and Ham B S 2005 *Phys. Rev.* A **71** 013821
[6] Wu J-H, Raczyński A, Zaremba J, Zielińska-Kaniasty S, Artoni M and la Rocca G 2009 *J. Mod. Opt.* **56** 768
[7] André A and Lukin M D 2002 *Phys. Rev. Lett.* **89** 143602
[8] Artoni M and la Rocca G C 2006 *Phys. Rev. Lett.* **96** 073905
[9] Bajcsy M, Zibrov A S and Lukin M D 2003 *Nature* **426** 638
[10] Moiseev S A, Sidorova A I and Ham B S 2014 *Phys. Rev.* A **89** 043802
[11] Brown A W and Xiao M 2005 *Opt. Lett.* **30** 699
[12] Ling H Y, Li Y-Q and Xiao M 1998 *Phys. Rev.* A **57** 1338
[13] Su X M, Zhuo Z C, Ham B S and Kim J B 2007 *J. Korean Phys. Soc.* **51** 48
[14] Paspalakis E and Knight P L 2001 *Phys. Rev.* A **63** 065802
[15] Liu C, Gong S, Cheng D, Fan X and Xu Z 2006 *Phys. Rev.* A **73** 025801
[16] Boyd R W 1992 *Nonlinear Optics* (London: Academic)
[17] Jiang K J, Deng L and Payne M G 2006 *Phys. Rev.* A **74** 041803
[18] Jiang K J, Deng L and Payne M G 2007 *Phys. Rev.* A **76** 033819
[19] Jiang K J, Deng L, Hagley E W and Payne M G 2008 *Phys. Rev.* A **77** 045804
[20] Li R B, Deng L and Hagley E W 2013 *Phys. Rev. Lett.* **110** 113902
[21] Arkhipkin V G and Myslivets S A 2009 *Phys. Rev.* A **80** 061802
[22] Arkhipkin V G and Myslivets S A 2013 *Phys. Rev.* A **88** 033847
[23] Arkhipkin V G and Myslivets S A 2014 *Opt. Lett.* **39** 3223
[24] Arkhipkin V G and Myslivets S A 2016 *Phys. Rev.* A **93** 013810
[25] Rautian S 2008 *Opt. Spectrosc.* **104** 112
[26] Karpov S Y and Stolyarov S N 1993 *Phys.-Usp.* **36** 1
[27] Milonni P W 2005 *Fast Light, Slow Light and Left-Handed Light* (New York: Taylor & Francis Group)
[28] Manga Rao V S C, Dutta Gupta S and Agarwal G S 2004 *Opt. Lett.* **29** 307